

Molecular Subgroups of Glioblastoma– an Assessment by Immunohistochemical Markers

Ádám Nagy¹ · Ferenc Garzuly² · Gergely Padányi² · Iván Szűcs³ · Ádám Feldmann⁴ · Balázs Murnyák⁵ · Tibor Hortobágyi⁵ · Bernadette Kálmán^{1,2}

Received: 8 May 2017 / Accepted: 15 September 2017 / Published online: 26 September 2017
© Arányi Lajos Foundation 2017

Abstract Comprehensive molecular characterization of and novel therapeutic approaches to glioblastoma have been explored as a result of advancements in biotechnologies. In this study, we aimed to bring basic research discoveries closer to clinical practice and ultimately incorporate molecular classification into the routine histopathological evaluation of grade IV gliomas. Integrated results of genome-wide sequencing, transcriptomic and epigenomic analyses by The Cancer Genome Atlas Network defined the classic, proneural, neural and mesenchymal subtypes of this tumor. In a retrospective cohort, we analyzed selected subgroup-defining molecular markers in formalin-fixed paraffin-embedded surgical specimens by immunohistochemistry. Quantitative and qualitative scores of marker expression were tested in hierarchical cluster analyses to evaluate segregations of the molecular subgroups, which then were correlated with clinical parameters including patients' age, gender and overall survival. Our study has confirmed the separation of molecular glioblastoma subgroups with clear trends regarding clinical correlations. Future analyses in a larger, prospective cohort using similar methods are expected to facilitate the development of a molecular

diagnostic panel that may complement routine histological work up and support prognostication as well as treatment decisions in glioblastoma.

Keywords Glioblastoma · Molecular subgroups · Translation · Clinical setting

Introduction

Glioblastoma is the most frequent primary malignant brain tumor in adults. The current standard of care includes surgical resection with wide margins, temozolomide and radiotherapy, but it only yields an overall median survival of 14.6 months, with a 5-year survival of 5% [1–3]. The majority, 90% of glioblastomas, are primary tumors arising “de novo”, while the remaining 10% of glioblastomas are secondary tumors developing from lower grade gliomas. The overall and the 5-year survival of primary glioblastomas are significantly worse than those of the secondary tumors [4].

According to the histopathological classification by the World Health Organization (WHO), glioblastoma is the most malignant, grade IV glioma characterized by cellular pleomorphism, mitosis, invasiveness, angiogenesis and necrosis. Glioblastoma stem cells likely play key roles in tumorigenesis [5]. Heterogeneity is one of the histological and molecular hallmarks of these tumors. Integrated results of genomic and transcriptomic studies by the Cancer Genome Atlas Network (TCGA) established that glioblastomas may be sorted into four molecular subgroups including the proneural, neural, classic and mesenchymal subtypes, and alterations in three main signaling pathways were emphasized [6–9]. Epigenetic analyses by the TCGA highlighted the existence of a glioma CpG island methylator phenotype (G-CIMP) in a proportion

✉ Bernadette Kálmán
bernadett.kalman@etk.pte.hu; kalman.bernadett@markusovszky.hu

¹ Faculty of Health Sciences, School of Graduate Studies, University of Pécs, Pécs, Hungary

² Markusovszky University Teaching Hospital, University of Pécs, 5. Markusovszky Street, Szombathely 9700, Hungary

³ St Borbála Hospital, Tatabánya, Hungary

⁴ Faculty of Medicine, Institute of Behavioral Sciences, University of Pécs, Pécs, Hungary

⁵ Department of Pathology, Division of Neuropathology, University of Debrecen, Debrecen, Hungary

of glioblastomas, which overlapped with the proneural subtype [10].

Correlation with clinical data revealed that the mesenchymal subgroup may have the worst outcome, while the proneural subgroup is characterized by a relatively better prognosis [6–8]. Mutations in the isocitrate dehydrogenase (*IDH*) genes, in addition to the G-CIMP epigenetic marks, define primarily the proneural subtype. The 2016 revision of the WHO classification recommends the incorporation of certain molecular markers into the histopathological classifications of gliomas, and as a first line of differentiation, suggests the determination of the *IDH* mutational status in glioblastomas, but without the incorporation of further TCGA subgroup-defining molecular markers in the diagnostic algorithm [11–14].

The genome-wide DNA, RNA and epigenome analyzes by TCGA were carried out in frozen glioblastoma samples. Neither this type of specimens nor the OMICS approaches can currently be used in clinical practice. Therefore, translational studies are needed to bring these research results closer to the clinical routine and test a selected set of key TCGA markers that may define the main molecular subgroups, predict prognosis and identify potential future treatment targets. In addition, such studies should be carried out in formalin-fixed, paraffin-embedded (FFPE) specimens and by using methods such as immunohistochemistry (IHC), fluorescence in situ hybridization (FISH) and sequencing available in regular pathology labs [15–18]. In the last few years, several groups have attempted the translation of research outcomes for clinical classification of glioblastomas, but no widespread adaptation of the results followed, leaving the opportunity open for further translational efforts [15–17, 19–23].

In the determination of glioblastoma molecular subgroups, gene expression alterations, somatic mutations, copy number variations and rearrangements are of particular importance. Based on the TCGA results, we have selected a few key markers for our translational study. This short list includes products of growth factor receptor, tumor suppressor and metabolic regulatory genes. A key growth factor receptor is the epidermal growth factor receptor (EGFR) that has increased expression due to amplification and several mutations with particular importance of the EGFRvIII mutation in glioblastomas [24]. The EGFRvIII mutants are characterized by deletions with various breaking points in individual tumors, which uniformly encompass the gene segment between exons 2 and 7, with a resultant protein product that is lacking the ligand binding site from the extracellular domain of the transmembrane receptor. This truncated receptor, however, is constitutively active (without the engagement of the receptor with its ligands, i.e. the epidermal growth factor [EGF]), and contributes to glioblastoma growth by EGFR-regulated DNA replication processes, pyrimidine and purine metabolism, and toll-like receptor (TLR) responses modulating apoptosis [24, 25].

The increased expression of EGFR and the presence of EGFRvIII are predominantly detectable in the classic molecular subtype [6–8].

Further important players in glioblastoma oncogenesis involve mutations in tumor suppressor genes that may also correlate with subgroup specification. One of the key tumor suppressor genes is the neurofibromin (*NF-1*) gene that may be affected by a large number of inactivating somatic point mutations and deletions of variable extensions. A common alteration is the complete deletion of the 17q11.2 region, which completely eliminates neurofibromin expression. When the *NF-1* gene is completely eliminated or inactivated, the processes controlled by it, such as the RAS GDP ↔ RAS GTP transformation will be downregulated, resulting in an upregulation of the MEK/ERK and the PI3K/AKT signaling pathways, which in turn, leads to increased cell proliferation, decreased apoptosis and extended tumor survival. *NF-1* mutations and deletions are common in the mesenchymal subgroup, usually associated with short overall survival and poor prognosis [6–8, 26–28].

Another key molecular marker for glioblastoma classification is the *IDH* mutation status that markedly influences the metabolic profile and impact on several regulatory mechanisms of the tumor [29]. The 2016 revision of glioma WHO classification suggests sorting of glioblastomas into two subgroups including those with *IDH-1* wild type (about 90% of cases that are usually older patients with primary glioblastomas) and those with *IDH-1* mutants (about 10% of cases that are usually younger patients with secondary glioblastomas) [14]. The most common *IDH-1* mutation is the R132H point mutation in glioblastoma, which renders the enzyme catalytically inactive [30]. Statistically, approximately 95% of secondary glioblastomas have this mutation, while it is present in only 4–6% of primary glioblastomas. The *IDH-1* R132H mutation causes abnormalities in the normal enzymatic function that is the oxidative decarboxylation of isocitrate into α -ketoglutarate, while it also leads to the accumulation of a metabolite, D-2-OH-glutarate (D2OHG). D2OHG has multiple alternative effects contributing to malignancy, therefore, it is called an oncometabolite [29]. This oncometabolite enhances the expression of the hypoxia-inducible factor (*HIF*)-1 α gene, activates cell cycle, contributes to telomere prolongation, epigenetically dysregulates a number of genes, while also impacts on DNA replication [31], activates the mTOR pathway and controls tumor cell migration [32].

In our study, we used markers selected from the list of the TCGA subgroup-defining molecules for the analyses of clinical FFPE glioblastoma specimens [6–8]. In our molecular cluster and clinical correlation analyses, the EGFR, EGFRvIII, *NF-1* and *IDH-1* R132H markers defined at the protein-level by IHC showed of particular utility for the glioblastoma subtype determination. These molecules were complemented by additional markers, such as p53, ATRX

and CD133, which seemed to be important in previous studies, but at the end, did not strengthen the outcome of our analyses [6, 7, 33–37]. We postulated that in case the subgroup determinant markers turn out to have biological relevance based on clinical correlations, the selected markers will forecast prognosis and highlight potential targets for future personalized therapies.

Aims of the Studies

We aimed to test a set of markers on retrospective FFPE glioblastoma specimens surgically obtained from 104 patients in the Department of Pathology of the Markusovszky University Teaching Hospital (MUTH), using methods of IHC and pyrosequencing, based on previously published molecular and biological subgroup results from genome-wide sequencing and transcriptomic analyzes in frozen glioblastoma samples by the TCGA. In case of a successful outcome, we plan to generate an algorithm with relatively few markers capable of efficiently and reproducibly separating the molecular, biologically relevant subgroups of glioblastoma tumors in the clinical practice.

Materials and Methods

Ethics Statement

The study has been approved by the institutional Ethics Board, and followed the ethical principles of research studies involving human subjects, as adopted in the Declaration of Helsinki.

Patients

One-hundred and twenty-seven surgically removed FFPE specimens from 112 patients with glioblastoma were collected and archived at the Pathology Department of the MUTH between 2000 and 2016. After reviewing the quality (e.g. extent of necrosis, integrity of tissue) and quantity (available tissue amount) of the specimens, 114 FFPE blocks of 104 patients were included in the study. In all cases, definite diagnosis of

glioblastoma was established by clinical, paraclinical and histological evaluations.

Table 1 shows the characteristics of patients. Of the 104 patients, 46 (44.23%) were male, and 58 (55.76%) were female. The age of onset ranged between 26 and 88 years; the mean age for the entire cohort was 61.01 years, the median 63.5 years. In the male subcohort, the onset age ranged between 26 and 77 years; the mean age was 58.89 years, the median 60 years. In the female subcohort, the age of onset ranged between 32 and 88 years; the mean age was 61.69 years, the median 65 years.

Our patient cohort was studied in two groups. The first group included 96 patients from whom specimens were available from the first surgery before chemo- and radiation therapy. While most tumors were unifocal, there were two multifocal glioblastomas (one with 2 foci, and another with 3 foci) among the specimens of this cohort. The second group included 8 patients with 18 specimens, where multiple (2 or more) specimens were obtained from the first and subsequent surgeries. In this group, only the first specimens (a total of 8) were obtained before chemo- and radiation therapy, while the second, third and fourth samples (a total of 10) were derived from recidive tumors, arising after chemo- and radiation therapies.

The majority of tumors, 101 samples were primary glioblastomas, but 3 secondary glioblastomas also were among the specimens of the total patient cohort of 104. Two secondary glioblastomas were in Cohort 1, while one secondary glioblastoma was in Cohort 2.

Immunohistochemistry (IHC)

IHC procedures were carried out according to the results of a technical pilot study that optimized the preanalytical steps and the dilutions of primary antibodies (Table 2). For visualization of the results, the secondary antibodies and DAB (diaminobenzidin) chemistry included in the Novolink Polymer Detection Systems RE-7140-K kit (Leica Biosystems, Newcastle, UK) were used according to the manufacturer's instructions, and was complemented by hematoxylin staining.

Table 1 Characteristics of patients and specimens

	Diagnosis glioblastoma		Gender		Type of surgery	
	Primary glioblastoma	Secondary glioblastoma	Males	Females	Resection	Biopsy
All patients	101	3	46	58	100	4
Cohort 1	94	2	43	53	93	3
Cohort 2	7	1	3	5	7	1

Table 1 indicates characteristics of the 104 patients and the two subcohorts (Cohort 1: 96 patients and Cohort 2: 8 patients) included in the study

Table 2 Specificities and technical characteristics of primary antibodies used in IHC

Specificities of primary antibodies	Clonality	Dilution	Antigen retrieval
GFAP	Monoclonal (mouse)	1: 100	5 min, 96 °C 0,01 M citrate buffer
NF-1	Polyclonal (rabbit)	1: 300	5 min, 96 °C 0,01 M citrate buffer
EGFR	Monoclonal (mouse)	1: 35	3 min, proteinase-K digestion
EGFRvIII	Polyclonal (rabbit)	1: 200	3 min, proteinase-K digestion
P53	Monoclonal (mouse)	1: 40	5 min, 96 °C 0,01 M citrate buffer
ATRX	Polyclonal (rabbit)	1: 500	10 min, 98 °C 0,01 M citrate buffer
IDH-1 R132H	Monoclonal (mouse)	1: 40	5 min, 96 °C 0,01 M citrate buffer
CD133	Monoclonal (mouse)	1: 300	7 min, 96 °C 0,01 M citrate buffer

Table 2 summarizes methodological characteristics of the monoclonal antibodies used in the IHC analyses

Using 1:50–1:100 magnification, region of interest (ROI) within each sample was selected based on evaluation of hematoxylin-eosin (H-E) and glial fibrillary acidic protein (GFAP) stained sections, which identified the most malignant appearing areas with dividing cells, pleomorphic nuclei, less angiogenesis, and no or minimal necrosis.

Three independent evaluators read the IHC results using 1:200 magnification under an Olympus BX51 microscope (Olympus Corp. Japan). The staining intensity score was defined as 0, +, ++ or +++, and the percentage of positive cells was determined in three microscopic fields. Histoscore values were generated by multiplying the staining intensity score with the % of positive cells.

Pyrosequencing

IHC assessments of the IDH-1 R132H mutants by mutant-specific monoclonal antibody were confirmed by pyrosequencing. First, sections prepared from the FFPE blocks were deparaffinized by using a QiaGen® Deparaffinization Solution for FFPE samples kit, then DNA was isolated by using a QiaGen® QIAamp DNA FFPE Tissue Kit (Qiagen Inc., Germantown, MD, USA). Concentration and quality of the DNA specimens were determined by using the Thermo Scientific® NanoDrop 2000 machine equipped with the NanoDrop2000/2000c software.

The polymerase chain reaction (PCR) was run with DNA template adjusted to 1 ng/μl concentration in a BOECO Thermal Cycler TC – SQ (Boeckel + Co (GmbH + Co), Hamburg, Germany). PCR primers were synthesized based on previously published sequences and used at a final concentration of 25 ng/μl [30]. After completing forty PCR cycles, the amplified DNA products were checked by agarose gel electrophoresis.

Pyrosequencing was carried out using also a published primer sequence [30] on a PyroMark® Q24 equipment (Qiagen Inc., Germantown, MD, USA).

Statistics

In Cohort 1, hierarchical cluster analyses were used on quantitative and qualitative IHC data to identify important biomarker cluster structures in determining disease membership. Cluster-based differences were evaluated using parametric ANOVA or Student's *t*-probe for normally-distributed continuous variables. Pearson's Chi-square analyses were used for nominal variables and Kruskal–Wallis tests were used for non-parametric data. The Cox proportional hazard model was applied for testing univariable and multivariable associations among demographic, clinical, survival and biomarker data of the patients. For data collection and statistical analyses the SPSS 23 software and R statistical environment (hclust package) were used.

Results

Evaluation of IHC

Reading of the IHC staining results included evaluation of 100–100 cells per sample in 3–5 microscopic fields of the previously selected ROI. The expressions of EGFR and EGFRvIII proteins were primarily expected on the cell membrane as experienced in the majority of samples. However, cytoplasmic and perinuclear staining patterns were also seen in a few samples. During the evaluation, we quantified only the cell membrane staining representing the EGFR proteins with best defined function.

The R132H IDH-1 protein is expressed in the cytoplasm. In each sample, cytoplasmic staining was seen and evaluated, except in one sample where an additional light nuclear staining was also noted, which we assumed to be background staining.

The NF-1 protein is normally expressed in the cytoplasm. In our specimens, four different staining patterns were noted with various combinations of cytoplasmic and nuclear staining patterns: cytoplasm + nucleus-; cytoplasm + nucleus +; cytoplasm- nucleus +; cytoplasm- nucleus-. In this study, the

total loss of NF-1 protein with cytoplasm- nucleus- staining was considered a “NF-1 negative” result.

In our specimens, the p53 and ATRX staining patterns were limited to the cell nuclei.

The CD133 protein is a trans-membrane protein, and it was indeed the predominant staining pattern we observed in our specimens, though with relatively scant occurrence. When an additional cytoplasmic staining was seen in a few samples, we attributed that to background staining and quantified only the cell membrane staining in each sample.

The inter-individual agreement of histoscore values (the staining intensity score multiplied by % of positive cells) for GFAP, EGFR, p53, ATRX and CD133 IHC varied between 80 and 100%. The manual evaluations of the EGFR and EGFRvIII stained slides were complemented by automated analyses using the QuantCenter software package on the 3D HisTech Mirax Scan device (3DHISTECH, Budapest, Hungary). In case of the EGFRvIII and IDH-1 R132H IHC, the presence or absence of mutations (positive or negative status) was determined.

Evaluation of Pyrosequencing

The IDH-1 R132H mutation specific IHC staining results were confirmed by pyrosequencing. This analysis established that the “++” or higher staining intensity of IHC-positive cells are indeed cells carrying this mutation. Therefore, the IHC results with “+” or less intensity of IDH-1 R132H staining were deemed negative.

After we verified and cleaned all the quantitative histoscore values (for EGFR, NF-1, ATRX, p53, CD133) and qualitative mutant / non-mutant designations (for EGFRvIII and IDH-1 R132H) of the investigated proteins, we tabulated the results in a master file for statistical testing. For NF-1, we eventually used the observed four staining patterns (cytoplasm +, nucleus-; cytoplasm +, nucleus+; cytoplasm-, nucleus+; cytoplasm-, nucleus-) in the analyses.

Hierarchical Cluster Analyses of Molecular Data for Glioblastomas in Cohort 1

Separation of the molecular subgroups identified by the hierarchical cluster analysis can be illustrated by a “tree” arrangement complemented with the *p*-values (Fig. 1). We have evaluated several “statistical trees” with sequential evaluation of marker group segregation, and found the one in Fig. 1 statistically the most powerful representation of subgroup formation. Here, the first step involved the isolation of IDH-1 R132H positive (“1”) and negative (“0”) subgroups, where ten persons (11.11%) were positive, and 86 persons (89.89%) were negative for this marker (*p* = 0.001, 95% confidence level).

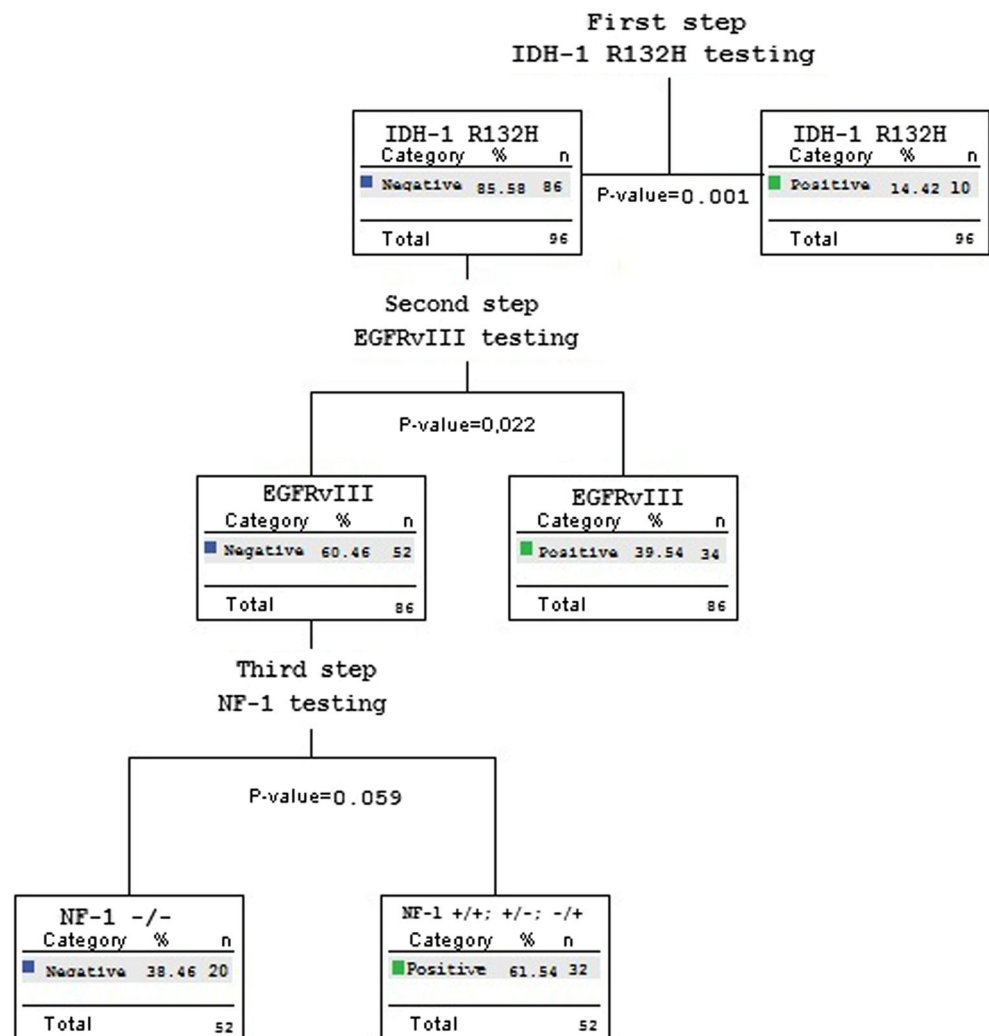
In the next step, we further divided the IDH-1 R132H “0” (negative) group based on the EGFRvIII mutation status for positive (“1”) and negative (“0”) subgroups. Out of 86 IDH-1 R132H negative patients, 32 persons (37.21%) were positive and 54 person (62.79%) negative for the EGFRvIII mutation. (Out of the total 96 patients, 33.33% was positive and 66.66% negative for the EGFRvIII mutation). There was no overlap in the EGFRvIII and IDH-1 R132H IHC staining in any patients included (*p* = 0.022, 95% confidence level).

Individuals falling in to the division of the “tree” where both the IDH-1 and EGFRvIII staining was negative (“0”) (Fig. 1), were further tested for the four expression patterns of NF-1 (NF-1 cytoplasm + nucleus -; NF-1 cytoplasm + nucleus+; NF-1 cytoplasm- nucleus+; NF-1 cytoplasm- nucleus-). Out of the EGFRvIII negative (“0”) subgroup, the separation of the NF-1 cytoplasm- nucleus- subgroup was near complete and approached (but with the reduced number of only 20 specimens in this subgroups, did not fully reach) significance (*p* = 0.059, 95% confidence level) (Figs. 1, 2 and 3). The three NF-1 positive variant patterns were observed in both the EGFRvIII positive (“1”) and negative (“0”) subgroups. The separation of each of these three NF-1 positive (including the cytoplasm + nucleus-, the cytoplasm + nucleus + and the cytoplasm-, nucleus+) subgroups was far from impressive and did not reach significance.

Based on the coexpression of EGFR and EGFRvIII mutation, expression of IDH-1 R132H mutation and the loss of NF-1 expression (cytoplasm-, nucleus-), we could sort 2/3rd of our glioblastoma specimens into three molecular subgroups (Figs. 2 and 3). The inclusion of additional IHC markers (p53, ATRX, CD133) either one-by-one or together in the hierarchical cluster analyses resulted in no further improvement of the subgroup separation.

Thus, based on the results of the above four marker expression, a statistically significant separation of the glioblastoma molecular subgroups was observed. The EGFR over-expression and the simultaneous presence of EGFRvIII mutation were identified in the largest subgroup (34 patients), which overlaps with TCGA classic subgroup [7, 8] and represents 35% of our cohort. The loss of nuclear and cytoplasmic NF-1 expression was detected in 20 samples, which may at least in part, be related to the TCGA mesenchymal subgroup [7, 8] and represents 21% of the total number of our samples. These two subgroups overlapped by 2 samples, wherein an increased EGFR and EGFRvIII expression was detected in addition to the loss of NF1 expression. These 2 patients represent only 2% of the total sample cohort. Finally, the IDH-1 R132H positive samples fully separated from the two former subgroups and likely correspond to the TCGA proneural category [7, 8]. This subgroup includes 10 patients, representing 10% of the total cohort (Figs. 2 and 3).

Fig. 1 A representative tree from the hierarchical cluster analyses. Figure 1 depicts segregation of subgroups in the hierarchical cluster analysis with the *p*-values indicated in between the branches. The architecture of the classification scheme can be read from top to bottom to see the sequential steps of the analysis



The Correlation of Clinical Outcomes with the Molecular Subgroups in Cohort 1

Out of the 96 patients involved in this retrospective study, clinical information could be recovered for 64 patients, and included the patients' gender, age at the diagnosis (surgery of glioblastoma) and overall survival time. The overall survival time was expressed in weeks, calculated from the date of surgery to the date of death. Three patients were still alive at the time of manuscript preparation. The clinical data were correlated with the molecular subgroups.

For testing the gender distribution in and among the subgroups, the Pearson's Chi-square test was used. Although some subgroups had rather small size, we can conclude that the patients' gender neither correlated with the overall survival time, nor with the molecular subgroups of the tumor (Table 3).

Next we tested the age of onset (age of glioblastoma diagnosis) in the molecular subgroups using Kruskal-Wallis test, but no significant *p*-values were obtained here either. Nevertheless, we recognized a certain trend: the age of

patients with the IDH-1 R132H mutation was 5–9 years younger than that in the other molecular subgroups. The mean age was 56 years and the median age of 52.5 years in the subgroup with IDH-1 R132H mutation, while the mean age was 62 years and the median 65 years in the IDH-1 R132H negative subgroups (Table 3).

Finally, we compared the overall survival of patients in the molecular subgroups using Cox regression analyses. These analyses also yielded non-significant results ($p = 0.386$), but again some of the molecular subgroups were too small. Nevertheless, some trends could be observed. The overall survival time was approximately 30 weeks longer in the IDH-1 R132H mutation positive subgroup as compared to the IDH-1 R132H negative (EGFRvIII+ and NF-1 -/-) subgroups. The mean value of overall survival times in the IDH-1 R132H mutant subgroup was 82 weeks, while it was only 50 weeks in the IDH-1 R132H negative cohorts. Similarly, the median survival time values appeared longer in the IDH-1 R132H mutation positive than in the negative subgroup (24 vs. 17 weeks, respectively) (Table 3). No differences in the

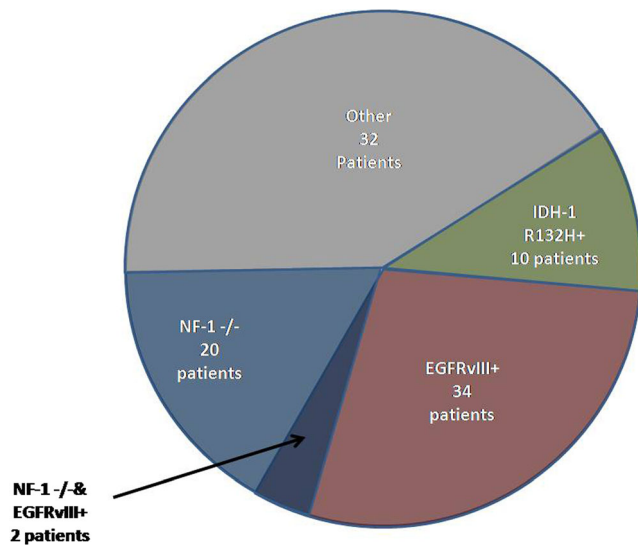


Fig. 2 Distribution of patients according to the key molecular markers. Figure 2 indicates the number of patients in the three main groups defined by the complete (cytoplasmic and nuclear) loss of NF-1 expression (blue), EGFR and EGFRvIII co-expression (red) and R132H IDH-1 mutation (green). The subgroup labeled by ““Other”” (gray) represents approximately 1/3rd of all patients, namely those who did not fall in the three key marker groups

survival time were observed in the other two molecular subgroups (EGFRvIII positive and NF-1 -/-) when compared with each other and with the IDH-1 R132H subgroup.

We also looked at the clinical characteristics according to the positive / negative status for EGFRvIII and NF-1 expression. (The comparison of survivals in the IDH-1 R132H positive and negative individuals is the same as above in the analyses in the molecular subgroups). The NF-1 positive

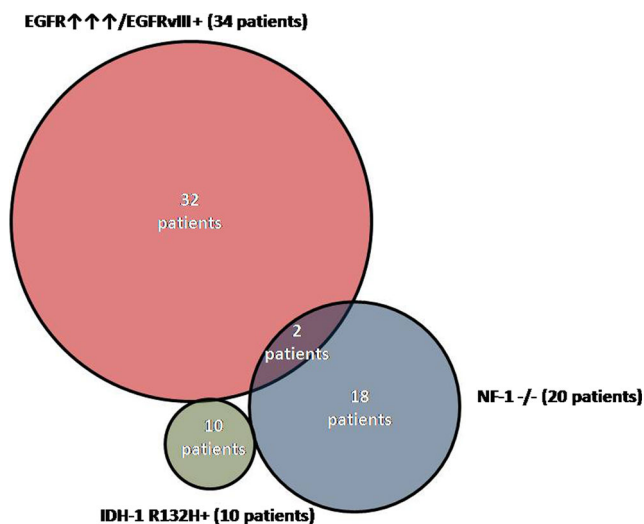


Fig. 3 Segregation of glioblastoma tumors into three molecular subgroups. Figure 3 shows the segregation of main molecular glioblastoma subgroups defined by the three key markers (complete loss of NF-1 expression, presence of IDH-1 R132H mutation and co-expression of EGFR upregulation along with the presence of the EGFRvIII mutation)

cohort (cytoplasm + nucleus-; cytoplasm + nucleus+; cytoplasm- nucleus+) had a mean age of 59 years, median age of 64, while the NF-1 negative cohort (cytoplasm- nucleus-) had a mean age of 65 years, median age of 67 years ($p = NS$). The mean survival time in the NF-1 positive group was 35 weeks, median 28 weeks, while the mean survival time was 50 weeks, median survival time 17 weeks in the NF-1 negative group ($p = NS$).

The EGFRvIII positive and negative cohorts did not differ in gender and age at diagnosis (mean age of 60 years vs. 61 years, median age of 65 vs. 61 years, respectively). The overall survival data of EGFRvIII + group appears slightly shorter than the EGFRvIII- group (mean 50 weeks vs. 61, median 22 weeks vs. 26 weeks), but this was not statistically significant by Cox regression analysis.

Molecular Profile Comparisons in the Sequential Glioblastoma Specimens in Cohort 2

This segment of the studies involved 8 patients with 2 or 3 surgical resections over time. Slides were prepared for IHC from FFPE blocks of resected tumors similar to that detailed above. Staining patterns of the first, second and when available, third / fourth samples were compared (Table 4). Since this was a very small sample size, we could not conduct statistical analyses. Nevertheless, Table 4 suggests that the molecular patterns did not profoundly change during the sequential sampling, even though some changes did occur. For example, in one case (patients 4), we noted a change in the NF-1 status when the first sample was negative, while the second sample was positive for this marker expression. There was no gross qualitative change in the expression of EGFR and EGFRvIII, however, in some samples we noted a quantitative increase as measured by the histoscore of EGFR expression over time. It is also worth mentioning that while ATRX was detected in the primary samples of 8 patients, 3 of them lost the ATRX expression over time (patients 1, 2 and 5). However, the reverse was true for patient 8. The rest of the IHC staining results showed no changes between the first and subsequent samples, suggesting that at least to some degrees, the molecular profiles of glioblastoma specimens are retained over time.

Discussion

In this study, 6 markers that showed key importance in the differentiation of glioblastoma molecular subgroups in previous research reports were selected for analyses in the clinical setting. These markers were studied in archived FFPE glioblastoma tumors by IHC method used in routine histopathology labs. In Cohort 1, we examined the separation of specimens based on the quantitative and qualitative

Table 3 Clinical characteristics of patients in the three molecular subgroups in Cohort 1

Mutations	Gender distribution	p-values Chi-square test	Mean age in years	Median age in years	p-value of Kruskal-Wallis test	Mean survival in weeks	Median survival in weeks	p-value of Cox-regression
IDH-1R132H	3 males 7 females	0.34	56	52.5	0.168	82	24	0.386
EGFR/EGFRvIII	15 males 19 females	0.93	60	61		50	22	
NF-1 +/-	11 males 9 females	0.28	65	67		50	17	

Table 3 summarizes distribution of the clinical characteristics (gender, age, overall survival) in the three molecular subgroups

expression of the 6 molecular markers, and investigated the correlation of clinical parameters with the marker-defined subgroups.

We conclude, that even with a few markers selected from the TCGA OMICS reports, identification of main glioblastoma molecular subtypes is feasible in clinical FFPE blocks (Figs. 1, 2, and 3). Based on the selected markers, an overlap between the IHC-defined and the TCGA-defined (proneural, classic and mesenchymal) subgroups is highly likely. Our results not only reproduce the separation of molecular subgroups in clinical glioblastoma specimens, but the distributions of these molecular subgroups are also similar to that reported by the TCGA network [6, 7]. Our results are also in consensus with earlier works of other authors regarding marker identity, subgroup separation and proportion, and some

clinical correlations, though the latter point requires further confirmation in our studies [9, 15, 17, 23, 38].

In our study, the patients' gender did not show differential distribution in the molecular subgroups of glioblastoma, and did not show any relationship to age of disease onset or overall survival. In contrast, we noted a strong tendency for longer survival associated with the IDH-1 R132H mutant status, as expected. Patients with this somatic mutation in their tumors also appeared younger at the disease onset, in concordance with the TCGA data [7]. However, as only 10 patients had glioblastoma with this mutation, no statistically significant *p*-values were detected in the correlation analyses due to lack of power.

In Cohort 2 including eight patients, we were able to examine more than one tumor specimen obtained at first

Table 4 Molecular characteristics of sequentially obtained glioblastoma specimens in Cohort 2

Patients	NF-1 +/-	EGFR membrane HistoScore	EGFRvIII +/-	IDH-1 +/-	p53 nucleus HistoScore	ATRX nucleus HistoScore
Patient 1 / 1st sample	-	n.e.	+	-	136	70
Patient 1 / 2nd sample	-	81	+	-	174	0
Patient 2 / 1st sample	+	156	+	-	186	80
Patient 2 / 2nd sample	+	176	+	-	62	0
Patient 3 / 1st sample	+	0	-	-	0	216
Patient 3 / 2nd sample	+	180	-	-	216	12
Patient 4 / 1st sample	-	249	+	-	237	98
Patient 4 / 2nd sample	+	273	+	-	174	216
Patient 5 / 1st sample	+	150	+	-	126	18
Patient 5 / 2nd sample	+	79	+	-	276	0
Patient 6 / 1st sample	+	76	+	-	237	195
Patient 6 / 2nd sample	+	234	+	-	60	148
Patient 7 / 1st sample	+	234	+	-	228	32
Patient 7 / 2nd sample	+	152	+	-	118	87
Patient 8 / 1st sample	+	150	+	-	159	0
Patient 8 / 2nd / a sample	+	264	+	-	213	0
Patient 8 / 2nd / b sample	-	210	n.e.	-	216	156
Patient 8 / 3rd sample	+	255	+	-	172	152

Table 4 shows molecular characteristics of multiple tumors obtained from eight patients with glioblastoma. From patient # 8 four surgical specimens were obtained at three time points, where 2 samples were taken at the second time point from the multi-focal tumor. HistoScore values are indicated for EGFR, ATRX and p53, while the presence of absence of mutation is indicated for IDH-1 R132H and EGFRvIII. Finally, four possible detection of NF-1 expression is shown with “-” representing nuclear-, cytoplasm- staining, while “+” representing all the other 3 possibilities including nuclear +, cytoplasm+; nuclear-, cytoplasm+; and nuclear+, cytoplasm + staining patterns

diagnosis and at recurrence(s) by surgical resections. This small substudy, although not suitable for statistical testing, suggests that glioblastoma tumors retain, at least in part, their main molecular characteristics over time. Nevertheless, our limited data also suggest the occurrence of some clonal changes as the somatic mutation profiles evolve in the tumors over time. However, sampling and intratumor heterogeneity may complicate the interpretation of these results as discussed in our previous reports [39, 40].

Our observations are in concordance with the 2016 revision of the WHO classification of gliomas which proposes the integration of molecular markers in the histopathology-based classification of these tumors, and the separation of glioblastomas for *IDH* mutation positive and negative subgroups [14]. Accordingly, the *IDH-1* R132 positive glioblastomas may be safely separated from the rest of glioblastomas, and represent the subgroup corresponding to the TCGA proneural subtype [7] (Figs. 1, 2 and 3). Both in the literature and our study, the *IDH-1* R132H positive status in great proportions (but not fully) meets the separation of primary and secondary glioblastomas (see also data in the [Introduction](#)).

While the 2016 revision of the WHO glioma classification does not recommend the inclusion of further markers in the glioblastoma molecular classification, our results suggest that the use of additional key markers are not only feasible, but also advisable for supporting clinical decision making. However, for the validation of our molecular observations and for a better definition of the clinical correlations, a prospective study with real-time collection of the clinical parameters along with the surgical tumor specimens will be necessary. Such study will provide a better insight into as to how the molecular glioblastoma subgroups differ from each other based on their biological properties. If we can reproduce the glioblastoma IHC-based subgroup separations, and establish the biological characteristics of the subgroups, we may proceed in the future in the direction of generating a molecular diagnostic panel for clinical practice to support prognosis and therapeutic considerations.

Finally, we need to make a note about the variations observed in IHC-detected protein expression patterns, often different from that expected in non-tumor brain tissue specimens. The aim of our studies was not to explore the genetic / genomic causes (somatic mutations and rearrangements) associated with the subcellular protein expression patterns in glioblastomas, nevertheless, we would like to call attention to a few points relevant for the study interpretation. The NF-1 protein is encoded in the chromosomal region 17q11.2, and is normally expressed in the cytoplasm, where it acts as an important tumor suppressor. The most common mutation affecting the *NF-1* gene in tumors is a complete loss of the long arm of chromosome 17, or deletions at the q11.2 region, which result in partial or complete loss of protein expression (loss of full protein or a specific epitope detectable by IHC). In addition,

numerous point mutations as well as smaller and larger insertions and deletions can occur which may affect the expression of the NF-1 protein, its subcellular localization and detectability by IHC [41–43]. Some mutations may cause retention of the mutated protein or protein segments in the nucleus. Missense and nonsense mutations may also alter epitopes of the NF-1 protein detectable by a given monoclonal antibody resulting in negative IHC. Background explorations of these changes at the protein level require comprehensive approaches, such as next generation sequencing and FISH analyses of the 17q11.2 region, or genome, exome and transcriptome level analyses. Although the TCGA database provides detailed information [6] regarding *NF-1* genotype - phenotype correlations, we have a small ongoing study to identify mutational events underlying the four observed expression patterns of the NF-1 protein.

IHC staining for EGFR and EGFRvIII has also produced some protein expression patterns in variance with the normal localization patterns. Predominantly, we observed staining of the cytoplasmic membrane as in normal cells, but in a small number of samples and in a few cells cytoplasmic and perinuclear staining was also observed. *EGFR* is encoded within the chromosome 7p13-q22 region [44]. In glioblastoma, the most common mutations are the copy number changes, especially amplification (detectable in approximately 30% of tumors), but deletion of the entire gene may also occur [24]. During mRNA processing and translation the receptor-related molecules travel through intracytoplasmic organelles to reach full maturation. Accordingly, the epitopes may be stained around the nucleus, but also within the cytoplasm (Golgi, endosomes, endoplasmic reticulum and even in the mitochondrion). Normally, these staining patterns do not or only scarcely occur. However, when the *EGFR* (and EGFRvIII) gene is amplified and the protein molecules are increased in number, intermediate products may be noted in unusual subcellular locations [45, 46]. Whether or not EGFR in such location exert any biological activity remains to be clarified.

Mutations in the *TP53* tumor suppressor gene are involved in promoting the growth and progression of several types of cancer. We have previously demonstrated the prognostic relevance of p53 expression in glioblastoma [47–50]. Normally, the protein is localized in the nucleus. This was also the case in our glioblastoma specimens. *TP53* is encoded in the 17p3 chromosomal region [51]. Deletion within this region or in the entire chromosome 17 may result in expression deficit of p53. Hot spots for point mutations include codons 175, 245, 248, 249, 273 and 282, which change the function or the isoform of the protein and its localization within the cell as well. Consequently, the molecule may appear in the cytoplasm instead of the nucleus, which we did not observe in our glioblastoma specimens [52–54].

Altogether, the strength of this study is that methods readily available in histopathology labs were used in archived clinical

FFPE glioblastoma specimens to test if main molecular subtypes of this tumor may be identified. This approach was capable of classifying 2/3rd of our glioblastoma specimens into molecular subgroups that likely overlap with the previously proposed TCGA subgroups, based on similar key markers. However, since this study included a retrospective cohort, clinical data could be retrieved only for 67% of the patients. Therefore, we had too small sample sizes per subgroups and lost statistical power in the clinical correlation analyses. Nevertheless, even with this limitation, we were able to observe certain trends, particularly for those tumors bearing the IDH-1 R132H mutation. Individuals with this mutation had an earlier age of disease onset and longer overall survival when compared to those lacking this IDH-1 R132H mutation. As an extension of the present study, we have a new study in progress with prospective specimen and clinical data collection to validate the glioblastoma molecular subgroups with biological characteristics. A successful outcome may lead to the generation of a clinical diagnostic panel for supporting prognosis and therapeutic considerations.

Acknowledgements These works were supported by an anonymous private donation and the University of Pécs internal and external funding systems. TH received support from the Hungarian Brain Research Programme (NAP KTIA_13_NAP-A-II/7) and GINOP-2.3.2-15-2016-00043. The present scientific contribution is dedicated to the 650th anniversary of the foundation of the University of Pécs, Hungary.

References

- Stupp R, Mason WP, Van Den Bent MJ, Weller M, Fisher B, Taphoorn MJ et al (2005) Radiotherapy plus concomitant and adjuvant temozolomide for glioblastoma. *N Engl J Med* 352(10):987–996
- Walker MD, Green SB, Byar DP, Alexander E Jr, Batzdorf U, Brooks WH et al (1980) Randomized comparisons of radiotherapy and nitrosoureas for the treatment of malignant glioma after surgery. *N Engl J Med* 303(23):1323–1329
- Laperriere N, Zuraw L, Cairncross G, Cancer Care Ontario Practice Guidelines Initiative Neuro-Oncology Disease Site Group (2002) Radiotherapy for newly diagnosed malignant glioma in adults: a systematic review. *Radiother Oncol* 64(3):259–273
- Chaurasia A, Park SH, Seo JW, Park CK (2016) Immunohistochemical analysis of ATRX, IDH1 and p53 in Glioblastoma and their correlations with patient survival. *J Korean Med Sci* 31(8):1208–1214
- Eidel O, Burth S, Neumann JO, Kieslich PJ, Sahm F, Jungk C et al (2017) Tumor infiltration in enhancing and non-enhancing parts of Glioblastoma: a correlation with histopathology. *PLoS One* 12(1):e0169292
- The Cancer Genome Atlas (TCGA) Research Network (2008) Comprehensive genomic characterization defines human glioblastoma genes and core pathways. *Nature* 455:1061–1068
- Verhaak RG, Hoadley KA, Purdom E, Wang V, Qi Y, Wilkerson MD et al (2010) Integrated genomic analysis identifies clinically relevant subtypes of glioblastoma characterized by abnormalities in PDGFRA, IDH1, EGFR, and NF1. *Cancer Cell* 17(1):98–110
- Brennan CW, Verhaak RG, McKenna A, Campos B, Noushmehr H, Salama SR et al (2013) The somatic genomic landscape of glioblastoma. *Cell* 155(2):462–477
- Aubry M, de Tayrac M, Etcheverry A, Clavreul A, Saikali S, Menei P et al (2016) From the core to beyond the margin: a genomic picture of glioblastoma intratumor heterogeneity. *Oncotarget* 6(14):12094–12109
- Noushmehr H, Weisenberger DJ, Diefes K, Phillips HS, Pujara K, Berman BP et al (2010) Identification of a CpG island methylator phenotype that defines a distinct subgroup of glioma. *Cancer Cell* 17(5):510–522
- Segerman A, Niklasson M, Haglund C, Bergström T, Jarvius M, Xie Y et al (2016) Clonal variation in drug and radiation response among Glioma-initiating cells is linked to proneural-Mesenchymal transition. *Cell Rep* 17(11):2994–3009
- He ZC, Ping YF, Xu SL, Lin Y, Yu SC, Kung HF et al (2015) Lower MGMT expression predicts better prognosis in proneural-like glioblastoma. *Int J Clin Exp Med* 8(11):20287–20294
- Myung JK, jin Cho H, Kim H, Park CK, Lee SH, Choi SH et al (2014) Prognosis of glioblastoma with oligodendroglioma component is associated with the IDH1 mutation and MGMT methylation status. *Transl Oncol* 7(6):712–719
- Louis DN, Perry A, Reifenberger G, von Deimling A, Figarella-Branger D, Cavenee WK et al (2016) The 2016 World Health Organization classification of tumors of the central nervous system: a summary. *Acta Neuropathol* 131(6):803–820
- Le Mercier M, Hastir D, Lopez XM, De Neve N, Maris C, Trepant AL et al (2012) A simplified approach for the molecular classification of glioblastomas. *PLoS One* 7(9):e45475
- Lee KS, Choe G, Nam KH, Seo AN, Yun S, Kim KJ et al (2013) Immunohistochemical classification of primary and secondary glioblastomas. *Korean J Pathol* 47(6):541–548
- Conroy S, Kruyt FA, Joseph JV, Balasubramanian V, Bhat KP, Wagemakers M et al (2014) Subclassification of newly diagnosed glioblastomas through an immunohistochemical approach. *PLoS One* 9(12):e115687
- Esteve-Codina A, Arpi O, Martínez-García M, Pineda E, Mallo M, Gut M et al (2017) A comparison of RNA-Seq results from paired formalin-fixed paraffin-embedded and fresh-frozen Glioblastoma tissue samples. *PLoS One* 12(1):e0170632
- Colman H, Zhang Z, Sulma EP, McDonald JM, Shooshtari NL, Rivera A et al (2010) A multigene predictor of outcome in glioblastoma. *Neuro-Oncology* 12(1):49–57
- Joseph NM, Phillips J, Dahiya S, Felicella MM, Tihan T, Brat DJ et al (2013) Diagnostic implications of IDH1-R132H and OLIG2 expression patterns in rare and challenging glioblastoma variants. *Mod Pathol* 26(3):315–326
- Chen L, Lin ZX, Li GS, Zhou CF, Chen YP, Wang XF et al (2015) Classification of microvascular patterns via cluster analysis reveals their prognostic significance in glioblastoma. *Hum Pathol* 46(1):120–128
- Denicola E, Tabouret E, Colin C, Metellus P, Nanni I, Boucard C et al (2016) Molecular heterogeneity of glioblastomas: does location matter? *Oncotarget* 7(1):902–913
- Cai J, Zhang C, Zhan W, Wang G, Yao K, Wang Z et al (2016) ATRX, IDH1-R132H and Ki-67 immunohistochemistry as a classification scheme for astrocytic tumors. *Oncoscience* 3(7–8):258–265
- Kalman B, Szep E, Garzuly F (2013) Post DE. Epidermal growth factor receptor as a therapeutic target in glioblastoma. *NeuroMolecular Med* 15(2):420–434
- Lindberg OR, McKinney A, Engler JR, Koshkaryan G, Gong H, Robinson AE et al (2016) GBM heterogeneity as a function of variable epidermal growth factor receptor variant III activity. *Oncotarget* 7(48):79101–79116

26. Vizcaíno MA, Shah S, Eberhart CG, Rodriguez FJ (2015) Clinicopathologic implications of NF1 gene alterations in diffuse gliomas. *Hum Pathol* 46(9):1323–1330
27. Xie B, Fan X, Lei Y, Chen R, Wang J, Fu C et al (2016) A novel de novo microdeletion at 17q11. 2 adjacent to NF1 gene associated with developmental delay, short stature, microcephaly and dysmorphic features. *Mol Cytogenet* 9(1):31–41
28. Way GP, Allaway RJ, Bouley SJ, Fadul CE, Sanchez Y, Greene CS (2017) A machine learning classifier trained on cancer transcriptomes detects NF1 inactivation signal in glioblastoma. *BMC Genomics* 18(1):127–128
29. Nagy A, Eder K, Selak MA, Kalman B (2015) Mitochondrial energy metabolism and apoptosis regulation in glioblastoma. *Brain Res* 1595:127–142
30. Setty P, Hammes J, Rothämel T, Vladimirova V, Kramm CM, Pietsch T et al (2010) A pyrosequencing-based assay for the rapid detection of IDH1 mutations in clinical samples. *J Mol Diagn* 12(6):750–756
31. Bardella C, Al-Dalahmah O, Krell D, Brazauskas P, Al-Qahtani K, Tomkova M et al (2016) Expression of Idh1 R132H in the murine subventricular zone stem cell niche recapitulates features of early Gliomagenesis. *Cancer Cell* 30(4):578–594
32. Zhu H, Zhang Y, Chen J, Qiu J, Huang K, Wu M, Xia C (2017) IDH1 R132H mutation enhances cell migration by activating AKT-mTOR signaling pathway, but sensitizes cells to 5-FU treatment as NADPH and GSH are reduced. *PLoS One* 12(1):e0169038
33. Yoon KS, Lee MC, Kang SS, Kim JH, Jung S, Kim YJ et al (2001) p53 mutation and epidermal growth factor receptor overexpression in glioblastoma. *J Korean Med Sci* 16(4):481–488
34. Liu Y, Wang F, Liu Y, Yao Y, Lv X, Dong B et al (2016) RNF135, RING finger protein, promotes the proliferation of human glioblastoma cells in vivo and in vitro via the ERK pathway. *Sci Rep* 6: e20624
35. Stieber D, Golebiewska A, Evers L, Lenkiewicz E, Brons NH, Nicot N et al (2014) Glioblastomas are composed of genetically divergent clones with distinct tumorigenic potential and variable stem cell-associated phenotypes. *Acta Neuropathol* 127(2): 203–219
36. Cancer Genome Atlas (TCGA) Research Network (2015) Comprehensive genomic characterization of head and neck squamous cell carcinomas. *Nature* 517(7536):576–582
37. Eckel-Passow JE, Lachanc DH, Molinaro AM, Walsh KM, Decker PA, Sicotte H et al (2015) Glioma groups based on 1p/19q, IDH, and TERT promoter mutations in tumors. *N Engl J Med* 372(26): 2499–2508
38. Olar A, Aldape KD (2014) Using the molecular classification of glioblastoma to inform personalized treatment. *J Pathol* 232(2): 165–177
39. Murnyák B, Csonka T, Klekner Á, Hortobágyi T (2013) Occurrence and molecular pathology of low grade gliomas. Alacsony grádusú gliális daganatok előfordulása és molekuláris patológiája. (in Hungarian) *Ideggyógyászati Szemle/Clinical Neuroscience* 66:305–311
40. Murnyák B, Csonka T, Hegyi K, Méhes G, Klekner Á, Hortobágyi T (2013) Occurrence and molecular pathology of high grade gliomas. (Magas grádusú gliomák előfordulása és molekuláris patológiája.) (in Hungarian) *Ideggyógyászati Szemle/Clinical Neuroscience* 66:312–321
41. McKeever PE, Dennis TR, Burgess AC, Meltzer PS, Marchuk DA, Trent JM (1996) Chromosome breakpoint at 17q11. 2 and insertion of DNA from three different chromosomes in a glioblastoma with exceptional glial fibrillary acidic protein expression. *Cancer Genet Cytogenet* 87(1):41–47
42. Vandenbroucke I, Van Oostveldt P, Coene E, De Paepe A, Messiaen L (2004) Neurofibromin is actively transported to the nucleus. *FEBS Lett* 560(1–3):98–102
43. Liu YC, Wang YZ (2015) Role of yes-associated protein 1 in gliomas: pathologic and therapeutic aspects. *Tumor Biol* 36(4): 2223–2227
44. Kondo I, Shimizu N (1983) Mapping of the human gene for epidermal growth factor receptor (EGFR) on the p13→ q22 region of chromosome 7. *Cytogenet Genome Res* 35(1):9–14
45. Lopez-Gines C, Gil-Benso R, Ferrer-Luna R, Benito R, Serna E, Gonzalez-Darder J et al (2010) New pattern of EGFR amplification in glioblastoma and the relationship of gene copy number with gene expression profile. *Mod Pathol* 23(6):856–865
46. Dasari VR, Velpula KK, Alapati K, Gujrati M, Tsung AJ (2012) Cord blood stem cells inhibit epidermal growth factor receptor translocation to mitochondria in glioblastoma. *PLoS One* 7(2):e31884
47. Csonka T, Murnyák B, Szepesi R, Kurucz A, Klekner Á, Hortobágyi T (2014) Poly(ADP-ribose) polymerase-1 (PARP1) and p53 labelling index correlates with tumour grade in meningiomas. *Folia Neuropathol* 52:111–120
48. Csonka T, Murnyák B, Szepesi R, Bencze J, Bognár L, Klekner Á, Hortobágyi T (2016) Assessment of candidate immunohistochemical prognostic markers of meningioma recurrence. *Folia Neuropathol* 54:114–126
49. Murnyák B, Kouhsari MC, Hershkovitch R, Kálmán B, Markovarga G, Klekner Á, Hortobágyi T (2017) PARP1 expression and its correlation with survival is tumour molecular subtype dependent in glioblastoma. *Oncotarget* 8(28):46348–46362. <https://doi.org/10.18632/oncotarget.18013>
50. Murnyák B, Hortobágyi T (2016) Immunohistochemical correlates of TP53 somatic mutations in cancer. *Oncotarget* 7:64910–64920
51. Masuda H, Miller C, Koeffler HP, Battifora H, Cline MJ (1987) Rearrangement of the p53 gene in human osteogenic sarcomas. *Proc Natl Acad Sci* 84(21):7716–7719
52. England B, Huang T, Karsy M (2013) Current understanding of the role and targeting of tumor suppressor p53 in glioblastoma multiforme. *Tumor Biol* 34(4):2063–2074
53. Smardova J, Liskova K, Ravcukova B, Kubiczikova L, Sevcikova S, Michalek J et al (2013) High frequency of temperature-sensitive mutants of p53 in Glioblastoma. *Pathol Oncol Res* 19(3):421–428
54. Kawasoe T, Takeshima H, Yamashita S, Mizuguchi S, Fukushima T, Yokogami K et al (2015) Detection of p53 mutations in proliferating vascular cells in glioblastoma multiforme. *J Neurosurg* 122(2): 317–323